



A Protection Strategy for an Electric Power Steering System powered by a Permanent Magnet Synchronous Motor

Ramy R. Sorial*, Mohammad H. Soliman, H. A. Talaat

Faculty of Engineering, Ain Shams University, Cairo, Egypt

Ramysorial92@gmail.com, mhsoliman76@eng.asu.edu.eg, hossam_talaat@eng.asu.edu.eg

Abstract A power steering system provides additional assist torque to the vehicle's driver, thus reducing the overall steering effort and providing a more comfortable driving experience. Electrically Assisted Power Steering (EAPS) uses an electric motor combined with a gearbox to provide the required assist torque. Performance and lifetime of such a system might be affected by how the driver is using it. Improper use might cause some parts to wear out and eventually need replacement, in some other cases the system might fail to operate. One of a such is caused by the impact of the steering rack with its mechanical travel limit. This paper presents a simulation of the Electrically Assisted Power Steering system through Matlab/Simscape using Field Oriented Control. In Addition, a solution to lower the intensity of such an impact by implementing a soft-limits algorithm inside the Electronic Control Unit (ECU). The proposed technique does not require any extra mechanical or electrical components.

Keywords Electrically Assisted Power Steering, Permanent Magnet Synchronous Motor, Field Oriented Control, Soft Limits

Introduction

Recently, automotive manufacturers were heading towards replacing complex mechanical systems with electrical ones, for example, Ignition control, Valve timing, Engine control, and management. Advantages of such an approach, other than cost and space optimization, are better control, ease of customization and the ability to implement more complex control strategies improving driving comfort and safety. In ground vehicles, the steering system plays a vital role in maintaining the motion trajectory of the car according to the driver's input and the existing road traffic [1]. Thanks to power steering, the need for a large steering wheel is no longer required allowing a better space utilization of the cockpit [2]. However, full-size vehicles are still equipped with hydraulic power steering since their steering system requires a large amount of power that the 12V system cannot supply [3]. The EAPS system uses an Electric Motor and a torque and angle sensor attached to the steering column to provide an assistance torque to the driver thus achieving a more comfortable driving experience. The challenges in this convention are to optimize the system's size, improve its dynamic performance while maintaining the same performance over the entire product lifetime. This was challenging since conventional DC motors (Brushed DC motors) had a poor life-time due to the wearing of the brushes, in addition to its poor dynamic performance, inadequate cooling and high operational noise. For this reason, a more reliable approach has been followed by using a Permanent Magnet Synchronous Motor (PMSM). PMSM offers a better lifetime, lower noise, smaller size and improved dynamic performance. However, it requires a more complex controller. Current literature in EAPS is focusing on optimizing system performance by achieving lower torque ripple as low as 1.5% [4], reducing its overall cost by using lower cost position sensors while maintaining low torque ripple [5] and improving its response in special cases such as return to center by



using active techniques [6]. The vehicle power steering system does not only affect the driving comfort but also affects the safety of the vehicle and its passengers. Failure in any of the steering system components may not only lead to an unpleasant driving experience but can also jeopardize the safety of the passengers on board. Since the EPAS mainly depends on electrical components (e.g., Electric motor, Control unit) in addition to the mechanical components, the failure can be caused by an electrical or a mechanical fault. Aside from sensor failure and wiring harness issues, overheating of the electrical components can be considered one of the main causes of failure. This case may occur in a stall condition where the driver is trying to rotate the steering wheel in the presence of a blocking obstacle. It may also happen if the driver is trying to turn the steering wheel after reaching its mechanical travel limit. So, the measurement of the electric motor and motor driver temperature is required to be able to protect the system from such failure. The obvious solution would be to add a temperature sensor inside the Electronic Control Unit (ECU) near the power switches and another one is placed inside the electric motor to sense the stator windings temperature. The main drawback of this technique, aside from the extra cost, is the possibility of sensor failure. For this reason, a more improved approach has been previously introduced by estimating the motor winding temperature using d-axis current injection [7]. The scope of this paper is the protection of the EAPS system’s mechanical and electrical components using active techniques that do not require any extra hardware to be installed. Instead of estimating or measuring the motor windings temperature, the system defines a set of operational limits that prevent the driver from overloading the system causing overheating and possibly damaging other parts. In order to test and evaluate the effectiveness of the proposed algorithm, a complete model of the EAPS system containing the simplified mechanical part as well as the electrical part controlling the behavior of the system has been built and simulated using Simulink/Simscape environment. The proposed algorithm is used to reduce the amount of assist when the steering rack is reaching its mechanical travel limit.

System Model

When the driver manipulates the steering wheel, he exerts torque on the steering column. Such torque is captured by a torque sensor mounted on the steering column. Information from the torque and angle sensors mounted on the steering column are fed into the Electronic control unit (ECU). The ECU then computes the required assist torque to be generated by the electric motor. Figure 1 represents the block diagram of the EAPS which will be discussed in detail in the next few sections.

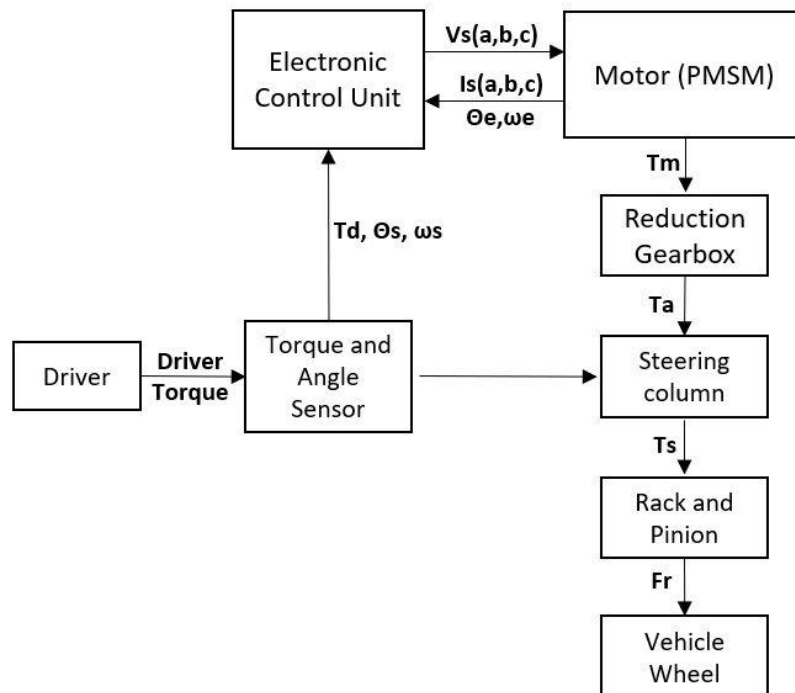


Figure 1: System Block diagram

Mechanical model

According to the motor location, EAPS systems can be classified into 3 main types: column assist, pinion assist and rack assist [8]. The mechanical system adopted in this paper is a column-assist type where the motor is connected to the steering column via a worm gearbox as shown in Figure 2.

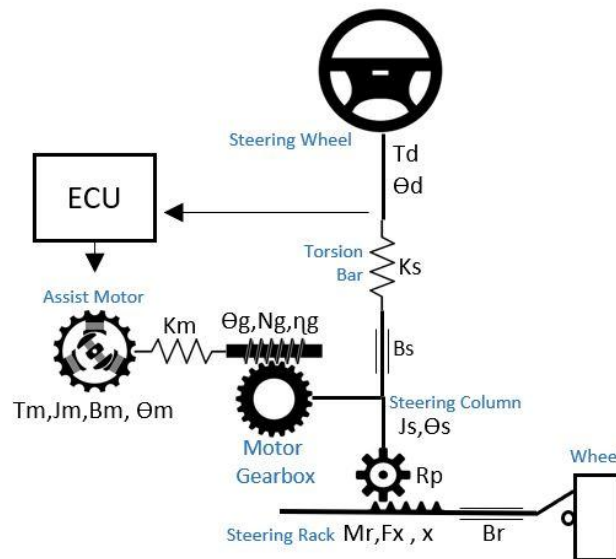


Figure 2: Mechanical System Block diagram

Torque-sensing is accomplished by measuring the angular deflection around the ends of the torsion bar. Torque from the steering wheel is summed with the generated assist torque and then fed to a rack and pinion system which converts rotary motion to linear motion pushing the steering rack in the desired direction. In the physical system, K_s represents the stiffness of the torsion bar used to sense the driver's applied torque, while K_m represents the torsional stiffness of the flexible coupling used to connect the motor shaft to the gearbox. The mechanical system parameters have been taken from [4], while the motor parameters have been taken from [5]. The rotary mechanical system dynamics are represented by the following equations:

$$T_s = T_d - J_s \ddot{\theta}_s - B_s \dot{\theta}_s + N_g I_g (T_m - J_m \ddot{\theta}_m - B_m \dot{\theta}_m) \tag{1}$$

$$\text{Where: } T_d = (\theta_d - \theta_s) K_s \tag{2}$$

$$\text{And: } T_m = (\theta_m - \theta_g) K_m \tag{3}$$

Where T_s is the steering column torque, T_d is the driver torque, T_m is the motor electromagnetic torque and J_s, B_s, J_m, B_m are the steering column inertia, steering column viscous friction coefficient, motor inertia, and motor viscous friction respectively. The resulting force F_x on the steering rack is calculated by the following equation:

$$F_x = \frac{1}{R_p} T_s - M_r \ddot{x}_r - B_r \dot{x}_r \tag{4}$$

Where R_p, M_r, B_r are the pinion gear radius, mass of rack and rack viscous friction respectively.

The mechanical system has been modeled using Matlab/Simscape physical model blocks allowing a bidirectional flow of energy between various system components. This gives the ability to study the effect of mechanical system dynamics on the motor and vice-versa.

Electrical Machine

The motor used in this paper is a 3-phase, 6-pole surface-mounted Permanent Magnet synchronous Motor (PMSM) [5]. The motor has a rated torque of 3.7 Nm at 1000 RPM and a rated current of 72 A. Thanks to the worm-type gearbox connecting the motor to the steering column, the system is able to provide a maximum assist torque of 62 Nm. The dynamic equations of the motor in the rotating reference frame are as follows:

$$V_d = R_s i_d + L_d \frac{d}{dt} i_d - \omega_e L_q i_q \tag{5}$$

$$V_q = R_s i_q + L_q \frac{d}{dt} i_q + \omega_e L_q i_q + \lambda_f \omega_e \tag{6}$$

$$\text{and } \omega_e = p \omega_m \tag{7}$$

Where ω_e , ω_m and p are the electrical angular velocity, mechanical angular velocity and number of pole pairs respectively. L_d, L_q are the direct and quadrature axis inductances, which in case of a cylindrical rotor are almost equal, and λ_f is the flux established by the rotor permanent magnets. The Resulting Electromagnetic torque is as follows:

$$T_e = \frac{3}{2} p \lambda_f i_q \tag{8}$$

Electronic Control Unit

The primary targets of electric power steering systems are to reduce the steering effort exerted by the driver and to improve the steering performance. The electronic control unit can be divided into three main parts: **Command estimator**, **Torque Controller**, and the **Inverter** as shown in Figure 3.

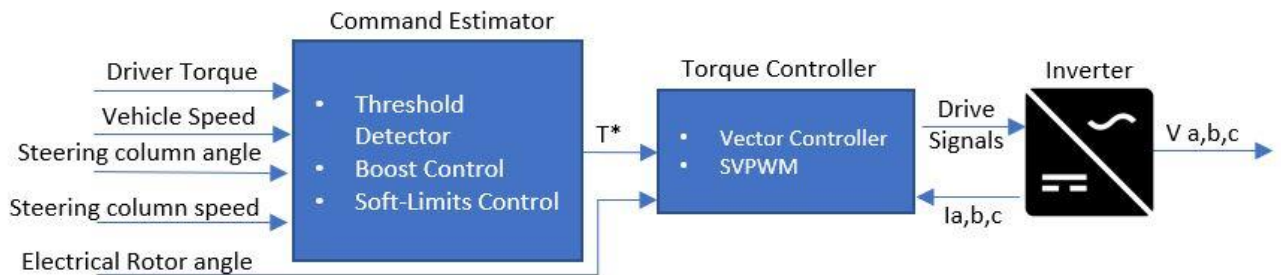


Figure 3: Electronic Control Unit block diagram

Torque Controller

Electrically Assisted Power Steering can be considered as a torque amplifier where the motor output torque depends on the driver’s input. The function of the torque controller in the system is to make sure the motor achieves the command torque value T^* calculated by the command estimator. For this reason, Field-Oriented Control is used to control the motor output torque since it directly controls the q-axis current which in-turn controls the motor’s electromagnetic torque. Using the information about the electrical rotor angle and stator currents, a voltage is generated and fed to the motor producing a magnetic flux orthogonal to the rotor’s magnetic flux. In Field Oriented Control, the system setpoint is the motor quadrature current I_q^* which corresponds to the command torque T^* coming from the command estimator according to the following relation:

$$I_q^* = T^* / K_t \tag{9}$$

$$K_t = \frac{3}{2} P \lambda_f \tag{10}$$

Where K_t , P and λ_f are the motor Torque constant in Nm/A , Number of pole pairs and permanent magnet flux in $V.s$. Direct current set point is set to zero since the rotor flux is generated by its permanent magnets. The actual direct and quadrature axis currents converted from stationary reference frame currents are compared to their references generating error signals which then drive two Proportional-Integral controllers. The output of the controllers is then fed to an SVPWM (Space Vector Pulse Width Modulation) controller to drive the inverter gates as shown in Figure 4. In addition to its lower harmonic distortion, SVPWM is capable of achieving better utilization of the DC link voltage compared to sinusoidal PWM [9]. Switching frequency is set to 20 KHz. Low switching frequency will cause operational noise and vibration, while high values will put an extra burden on the switching devices. A saturation block is used to limit the q-axis command current to the rated value of the motor which is (72 A).

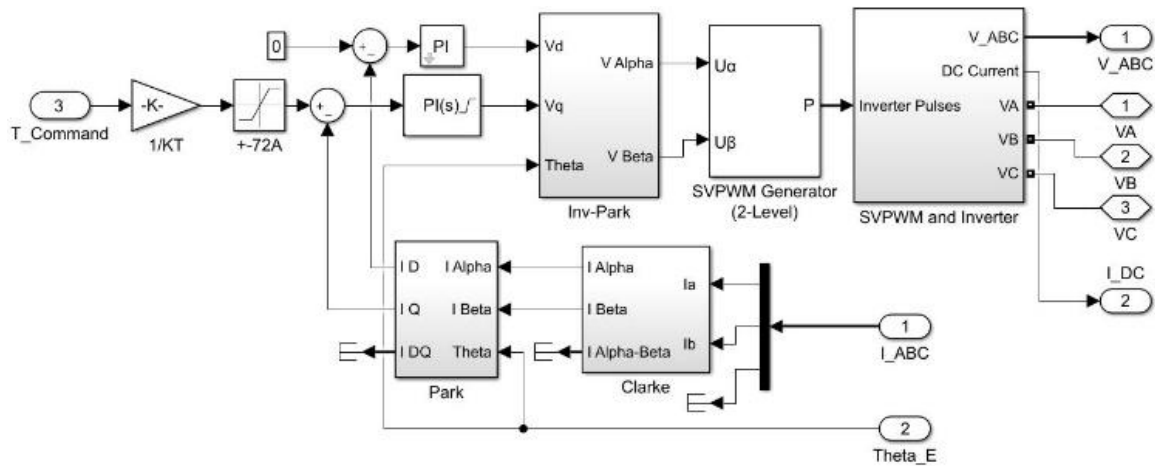


Figure 4: Torque Controller block diagram

Inverter

In order to drive the motor coils from a DC voltage source an inverter circuit is required. In this case a MOSFET inverter is used due to its high current sourcing capability and low ON resistance. As shown in Figure 5, gating signals from the torque controller are connected to the SVPWM output signals block.

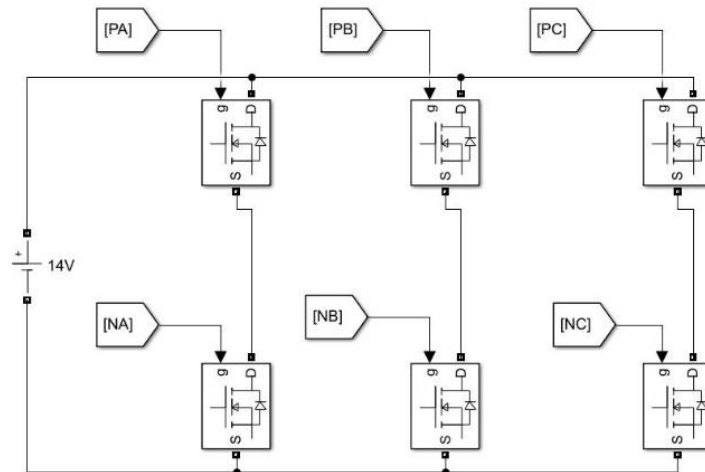


Figure 5: Inverter Block diagram

Although a vehicle’s battery voltage is 12 V, the DC bus voltage in the vehicle during normal operation is 14 V since this is the voltage generated and by the alternator to charge the battery and to supply the rest of the electrical loads in the vehicle.

Command Estimator

The function of the command estimator is to determine the amount of assist torque to be generated by the electric motor based on the driver’s applied torque, vehicle speed, and the steering wheel angle and rotational speed. The command estimator in this paper is divided into two main parts:

- Steering boost calculator
- Soft Limits generator

Steering Boost Calculator

Power assist characteristics curve (or Boost Curve) is a function of steering wheel torque and vehicle speed. There exist three types of boost characteristic curves: the straight-line type, fold line type and curve type [10]. Used in the paper is the straight-line type, featuring simpler calculations, requiring less computational power

compares to other types. Assist torque is mainly proportional to the driver’s applied torque. However, as the vehicle speed increases, the assist motor maximum torque is reduced till it reaches a certain speed where no assist torque is required. Assist torque command is inversely proportional to the vehicle speed. This is required since at higher vehicle speeds, less steering effort is required due to reduced tire-to-ground friction so less assist is required in order to maintain good road feel.

$$T^* \propto \frac{1}{V_s} \tag{11}$$

Where T^* is the assist torque command and V_s is the vehicle speed. As in [4], in order to improve system stability and avoid false triggering of the assist motor, a Threshold of $\pm 1 N.m$ is defined so that any applied torque within this region does not engage the assist motor, also any applied torque above $7 N.m$ sets the assist motor to output its maximum torque which is around $3.7 N.m$ at $72A$ resulting in a column assist torque of about $62 N.m$ (Taking into account various frictions and gearbox efficiency). Based on the driver input torque range and the maximum electromagnetic motor torque range. The following set of equations represent the piecewise linear relation between driver’s torque, vehicle speed and assist torque.

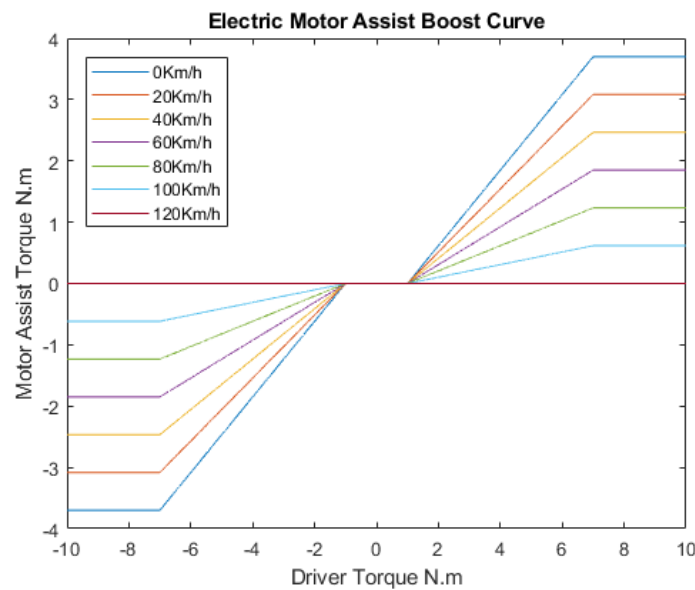


Figure 6: Steering boost curves

The assist slope is determined as follows:

$$Slope = \frac{T_{a(Max)}}{(T_{d(Max)} - T_{Offset})} \tag{12}$$

Where $T_{a(Max)}$ is the motor’s Maximum electromagnetic torque, $T_{d(Max)}$ is Maximum Driver applied torque and T_{Offset} is the Threshold torque in Nm. The effect of vehicle speed on the assist is calculated based on the Maximum speed above which steering assist is not required as follows:

$$G(v) = (v_{Max} - v) \frac{1}{v_{Max}} \tag{13}$$

Where v_{Max} and v are max vehicle velocity above which no assist is needed and the measured vehicle velocity respectively in Km/h. The Motor assist torque command T_a^* is defined as follows:

$$T_a^* = \begin{cases} 0 & |T_d| < 1Nm \\ F(T_d, v) & |T_d| \geq 1Nm \end{cases} \tag{14}$$

In case of driver torque above the maximum value, the assist equation is as follows:

$$F(T_d, v) = Slope * [T_d - (Sgn(T_d)T_{Offset})] * G(v) \tag{15}$$

$$T_a^* = \begin{cases} Sgn(T_d) * T_{m(Max)} & |F(T_d, v)| > G(v)T_{m(Max)} \\ F(T_d, v) & |F(T_d, v)| \leq G(v)T_{m(Max)} \end{cases} \tag{16}$$



Where T_d is the applied driver’s torque in Nm.

For a speed range of $0 \rightarrow 120 \text{ Km/h}$, Figure 6 demonstrates the motor electromagnetic torque command for various vehicle speeds showing a maximum assist at 0 Km/h and zero assist at 120 Km/h with an offset of 1 Nm and a maximum motor torque depending on the vehicle speed.

Soft Limits

The motion of the steering rack is governed by the existence of two hard limits placed on each side of the rack limiting the maximum wheel turning angle as shown in Figure 7. Those limiters are usually made from plastic materials such as nylon.

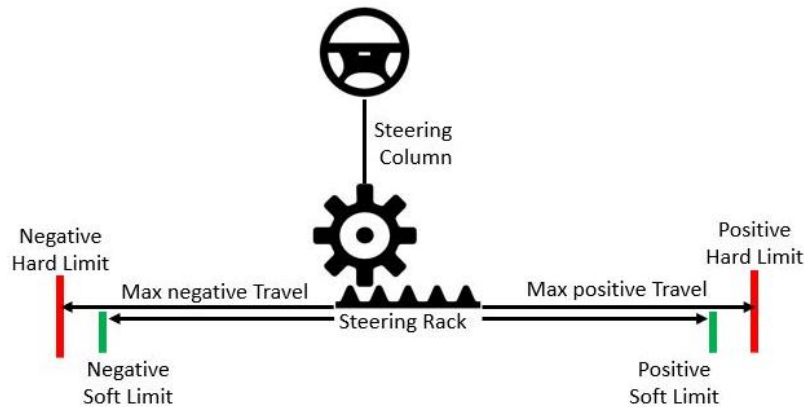


Figure 7: Mechanical and Soft Limits

When the wheel is rapidly rotated to its maximum angle in either direction, the steering rack will eventually bump into one of its mechanical hard limits. The impact will be transferred along the steering column to the steering wheel leading to an uncomfortable driving experience. Depending on how much torque was exerted from the driver, how much assist was provided, and how fast the steering wheel was turned at the time of the impact, permanent damage will eventually occur to the mechanical components of the steering system. This damage will have a significant impact on the steering performance which in turn affects the safety of passengers. Moreover, if the driver insists to apply torque in the direction of the reached hard limit, the motor coils and inverter switches will eventually overload. If no overheating protection algorithm is present, a permanent damage to the electrical system will occur. In order to simulate such an impact, a mechanical limit is placed in the way of the steering rack constraining its motion to 150 mm (a typical travel range for passenger vehicles) in both directions. Stiffness of the hard limit material about 10^9 N/m . The steering rack position is computed directly from the steering column angle using the following equation:

$$x_r = r_p \cdot \theta_s \tag{17}$$

Where r_p and θ_s are the radius of the pinion and the steering column angle respectively. When the rack position x_r reaches a value greater than the threshold position x_{th} , and the driver continues to rotate the wheel in the direction of the hard limit, the steering assist command value is decreased according to the below equation:

$$T_{out}^* = \begin{cases} T_{in}^* & \text{sgn}(T_{in}^* * x_r) < 0 \\ T_{in}^* \frac{x_{r(Max)} - x_r}{x_{r(Max)} - x_{th}} & \text{sgn}(T_{in}^* * x_r) > 0 \end{cases} \tag{18}$$

Where $x_{r(Max)}$ is the maximum physical travel of the rack. Figure 8 demonstrates the operation of the soft-limits algorithm:

In order to ensure proper engagement of the algorithm, soft-limits system is only activated when the driver’s torque is in the same direction where the threshold position is reached. This way, the driver gets normal assist when trying to rotate the steering wheel away from the hard limit. Soft-limits algorithm adds no extra cost to the system, since it does not require any external mechanical or electrical components. Moreover, the algorithm mainly depends on driver’s torque and steering wheel angular position which are basic parts of the EAPS system.

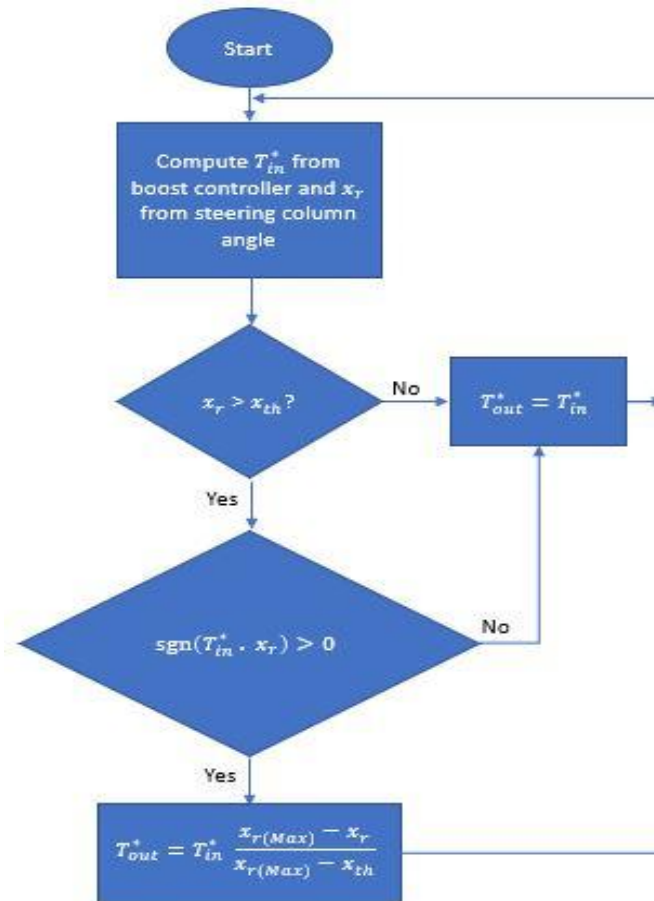


Figure 8: Soft limits flowchart

Simulation Results

A. System Response during normal operation

Figure 9 shows the system response when subjected to a sinusoidal input torque with an amplitude of 7.5Nm and a frequency of 5 rad/s. As the driver increases the applied torque, the boost controller increases the command torque. This represents the normal assist operation while the vehicle is at standstill (maximum assist). Assist command is fed to the torque controller (Field-Oriented Control) block which converts it to a quadrature axis current command. Command current is then fed to a Proportional-Integral (PI) controller which determines the appropriate stator voltage needed to achieve the required current. An SVPWM inverter is then used to drive the motor. Motor current command is limited to ± 72 A which is the rated current of the selected electric motor.

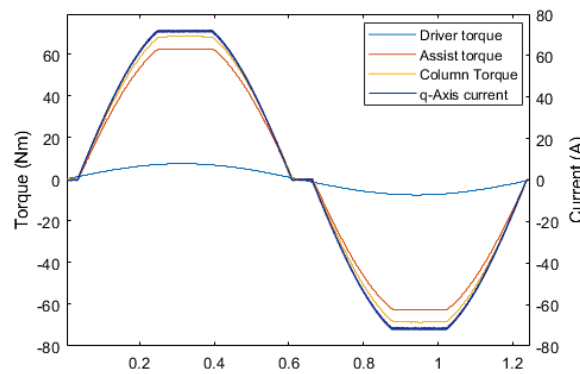


Figure 9: System Response under normal operating conditions



B. System response during mechanical impact

To simulate the impact of the steering rack with the mechanical motion limiter, a translational hard stop block from the SIMSCAPE toolbox was used, limiting the rack motion to $\pm 150\text{ mm}$. The motion threshold value in this simulation is set to $\pm 140\text{ mm}$ (10 mm before the hard limit). This means that when the rack position exceeds 140m, the amount of assist becomes inversely proportional to the rack position. Using this technique, the impact condition has been avoided since the ECU started to gradually decrease the amount of assist 10 mm before the hard limit. However, the driver still has full assist in the opposite direction since the algorithm is only engaged when the direction of the driver torque is the same as the steering wheel while heading towards its motion limit. The difference made by deploying the above technique can be observed through the below figures.

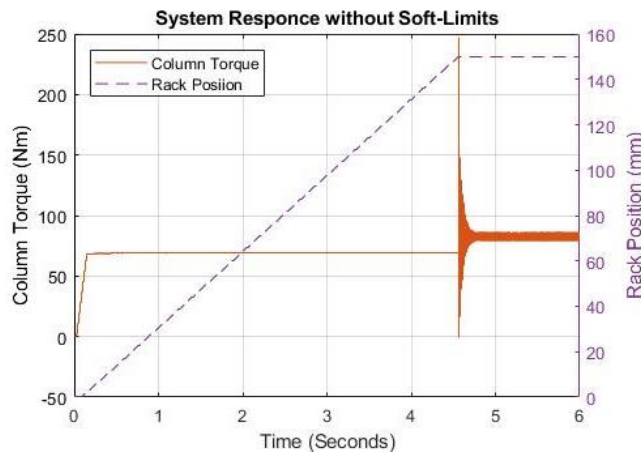


Figure 10: System response without soft-limits (7.5 Nm driver input)

As seen in Figure 10, in a traditional system without soft-limits, the resulting reaction torque generated from the impact of the rack with the hard limit is about 246 Nm which is 3.5 times higher than the normal operating value. When using the proposed algorithm, the intensity of the impact has been noticeably reduced as shown in Figure 11. This is because only the driver’s torque is present at this moment of impact.

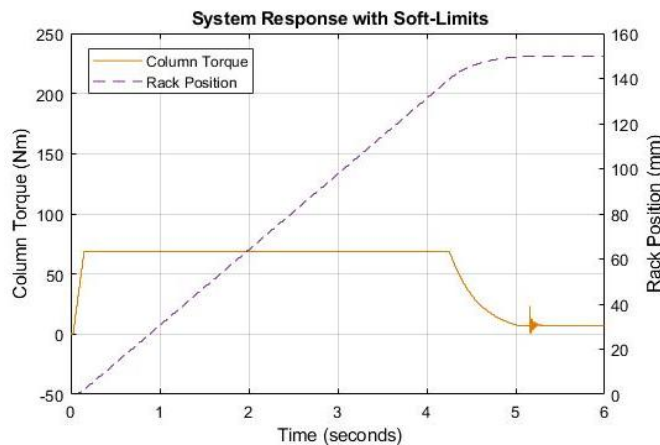


Figure 11: System response with soft-limits (7.5Nm driver input)

Besides, the gradual decrease applied by the algorithm in the amount of assist decreases the speed at which the rack approaches the hard limit. As a result, the impact is further damped. The benefit of such feature can be observed in the case when the driver exerts a higher torque in order to turn the wheel faster, or when the tire-to-ground friction is lower due to different types of terrain. Figure 12 shows the system responses when the tire-to-ground viscous friction is $2 \times 10^5\text{ N/(m/s)}$ and $1 \times 10^5\text{ N/(m/s)}$ respectively, driver input torque is 7.5 Nm in both cases. As seen from Fig. 12, the column torque at the moment of impact is still within its normal range.

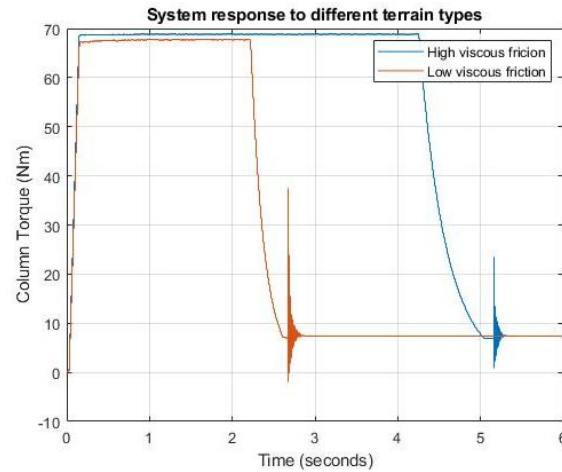


Figure 12: System response to different terrain types

Conclusion

EAPS offers better controllability and enhanced steering feel. However, due to the important role the steering system plays in the safety of the vehicle and its passengers, protection techniques are required to ensure proper operation over the entire product's lifetime. Using the proposed algorithm, the impact torque has been significantly reduced from 246 Nm to less than 30 Nm to fall within the normal operational value (0 to 69 Nm), thus ensuring a safer operation. Moreover, the algorithm does not interfere with the normal assist operation as long as the rack position is away from its limits. In addition, the gradual decrease in the assist ensures a comfortable and consistent steering experience. Yet, when rotating the wheel in the opposite direction, the driver instantly gets full assist ensuring good dynamic response. Furthermore, the technique discussed in this paper does not require any additional physical components to be added to the system. Instead, it uses information from the existing sensors to operate.

Acknowledgment

This work has been supported by the Electrical Power & Machines Department, Ain Shams University.

Appendix

Table 1: System Parameters

Parameter	Symbol	Value	Unit
Torsion Bar rigidity	K_s	200	Nm/rad
Column Viscous friction	B_s	0.26	$Nm/(rad/s)$
Column Inertia	J_s	0.012	$Kg.m^2$
Motor Coupling Rigidity	K_m	50	Nm/rad
Motor Inertia	J_m	0.00011	$Kg.m^2$
Motor Viscous Friction	B_m	0.00021	$Nm/(rad/s)$
Gearing Ratio	N_g	20	-
Gearbox Efficiency	Π_g	90	%
Pinion Radius	R_p	0.01	m
Mass of Rack	M_r	5.5	Kg
Rack Viscous Friction	B_r	653	$N/(m/s)$
Stator Resistance	R_s	0.023	Ω
D-Axis Inductance	L_d	68	μH
Q-Axis Inductance	L_q	68	μH
Pole pairs	P	3	-
Permanent Magnets Flux	λ_f	0.0109	$V.s$



References

- [1]. V. G. Nguyen, X. Guo, C. Zhang and X. K. Tran, "Parameter Estimation, Robust Controller Design and Performane Analysis for an Electric Power Steering System," MDPI, Algorithms, pp. 1-28, 2019.
- [2]. M. Chahare, M. I. Mhaisne and D. Dongre, "An Overview on Future Electric Steering System: A Project Approach," International Research Journal of Engineering and Technology (IRJET), vol. 4, no. 7, pp. 2152-2159, 2017.
- [3]. T. Mio, Y. Komatsubara, N. Ohmi, Y. Kimoto, K. Iizuka, T. Sukanuma, S. Maruyama, T. Sugiyama, F. Sato, S. Shinoda, T. Hibino and K. Nishi, "Auxiliary Power Supply System for Electric Power Steering (EPS) and High-Heat-Resistant lithium-Ion Capacitor," MDPI, World Electric Vehicle Journal, pp. 1-13, 2019.
- [4]. S. Guobiao, Z. Songhui and M. Jun, "Simulation Analysis for Electric Power Steering Control System Based On Permanent Magnetism Synchronization Motor," in 2nd International Conference on Electronic & Mechanical Engineering and Information Technology (EMEIT-2012), Shenyang, 2012.
- [5]. K.-Y. Cho, Y.-K. Lee, H. Mok, H.-W. Kim, B.-H. Jun and Y. Cho, "Torque Ripple Reduction of a PM Synchronous Motor for Electric Power Steering using a Low Resolution Position Sensor," Journal of Power Electronics, Vol. 10, No. 6, November 2010, vol. 4, no. 6, pp. 709-716, 2010.
- [6]. P.-P. Du, H. Su and G.-Y. Tang, "Active Return-to-Center Control Based on Torque and Angle Sensors for Electric Power Steering Systems," MDPI, Sensors, pp. 1-12, 2018.
- [7]. B.-S. Jun, J. S. Park, J.-H. Choi, K.-D. Lee and C.-Y. Won, "Temperature Estimation of Stator Winding in Permanent Magnet Synchronous Motors Using d-Axis Current Injection," MDPI, Energies, pp. 1-14, 2018.
- [8]. MR.R.G.Shirwastava and DR.M.B.Digavane, "Electric Power Steering With Permanent Magnet Synchronous Motor Used In Automotive Application," in International conference on Electrical Energy Systems (ICEES 2011), 3-5 Jan 2011, India, 2011.
- [9]. Maamoun, Y. M. Alsayed and a. A. Shaltout, "Space-Vector PWM Inverter Feeding a Permanent-Magnet Synchronous Motor," World Academy of Science, Engineering and Technology, International Journal of Electrical and Computer Engineering ,Vol:4, No:5, 2010, vol. 4, no. 5, pp. 829-833, 2010.
- [10]. Q. Liu, W. Kong and T. Li, "The Assist Curve Design for Electric Power Steering System," in 2nd International Conference on Advances in Mechanical Engineering and Industrial Informatics (AMEII 2016), China, 2016.

